

Unclassified

SECURITY CLASSIFICATION OF THIS PAGE

(2)

REPORT DOCUMENTATION PAGE

DTIC
REPRODUCED
FOR GOVERNMENT USE1a. REPORT SECURITY CLASSIFICATION
Unclassified

2a. SECURITY CLASSIFICATION

2b. DECLASSIFICATION

4. PERFORMING ORGANIZATION

Report 29

AD-A222 019

6a. NAME OF PERFORMING ORGANIZATION
Department of Chemistry
University of Florida6c. ADDRESS (City, State, and ZIP Code)
Department of Chemistry
University of Florida
Gainesville, FL 32611-20468a. NAME OF FUNDING/SPONSORING
ORGANIZATION
Office of Naval Research8c. ADDRESS (City, State, and ZIP Code)
800 N. Quincy St.
Arlington, VA 22217-5000

11. TITLE (Include Security Classification)

Ion/Molecule Reactions of Arsenic and Phosphorus Cluster Ions: Ionization Potentials and
Novel Reaction Pathways

12. PERSONAL AUTHOR(S)

Jeffrey A. Zimmerman, Stephan B. H. Bach, Clifford H. Watson, and John R. Eyler

13a. TYPE OF REPORT
Technical13b. TIME COVERED
FROM 10/89 TO 5/9014. DATE OF REPORT (Year, Month, Day)
1990, May 1815. PAGE COUNT
29.

16. SUPPLEMENTARY NOTATION

Submitted to the Journal of Physical Chemistry

17. COSATI CODES

FIELD	GROUP	SUB-GROUP

18. SUBJECT TERMS (Continue on reverse if necessary and identify by block number)

Arsenic clusters, Phosphorus clusters, Ionization potentials,
charge transfer reactions, Fourier transform ion cyclotron
resonance mass spectrometry. (JF)

19. ABSTRACT (Continue on reverse if necessary and identify by block number)

Ionization potentials (IP's) for arsenic and phosphorus clusters (As_n , $n = 1-5$; P_n , $n = 1-4$) have been determined by gas phase charge transfer reactions. Arsenic and phosphorus cluster ions were generated by pulsed CO_2 laser desorption from GaAs and InP substrates, mass selected, thermalized, and allowed to react with compounds of known ionization potential in a Fourier transform ion cyclotron resonance mass spectrometer. The IP's for As_3 and As_5 , previously unreported, as well as more accurate IP values for several of the other clusters, have been determined. Products and rate coefficients for some interesting reactions of the cluster ions with the charge transfer agents are also reported.

20. DISTRIBUTION/AVAILABILITY OF ABSTRACT

 UNCLASSIFIED/UNLIMITED SAME AS RPT. DTIC USERS

22a. NAME OF RESPONSIBLE INDIVIDUAL

Dr. David L. Nelson

21. ABSTRACT SECURITY CLASSIFICATION

Unclassified

22b. TELEPHONE (Include Area Code)

202-696-4410

22c. OFFICE SYMBOL

Office of Naval Research

Grant N00014-87-G-0248

R & T Code 4131007

TECHNICAL REPORT NO. 29

ION/MOLECULE REACTIONS OF ARSENIC AND PHOSPHORUS CLUSTER IONS:

IONIZATION POTENTIALS AND NOVEL REACTION PATHWAYS

Jeffrey A. Zimmerman, Stephan B. H. Bach,

Clifford H. Watson, and John R. Eyler

Submitted to

Journal of Physical Chemistry

University of Florida

Department of Chemistry

Gainesville, FL 32611-2046

May 19, 1990

Reproduction in whole or in part is permitted for any purpose of the United States Government.

This document has been approved for public release and sale; its distribution is unlimited.

Ion/Molecule Reactions of Arsenic and Phosphorus Cluster Ions: Ionization Potentials and Novel Reaction Pathways

Jeffrey A. Zimmerman, Stephan B.H. Bach,[†] Clifford H. Watson^{} and John R. Eyler^{*}**

*Department of Chemistry, University of Florida
Gainesville, Florida 32611-2046*

Abstract

Ionization potentials (IP's) for arsenic and phosphorus clusters (As_n , $n = 1-5$; P_n , $n = 1-4$) have been determined by gas phase charge transfer reactions. Arsenic and phosphorus cluster ions were generated by pulsed CO_2 laser desorption from GaAs and InP substrates, mass selected, thermalized, and allowed to react with compounds of known ionization potential in a Fourier transform ion cyclotron resonance mass spectrometer. The IP's for As_3 and As_5 , previously unreported, as well as more accurate IP values for several of the other clusters, have been determined. Products and rate coefficients of some interesting reactions of the cluster ions with the charge transfer agents are also reported.

^{*} Present Address: Chemistry Division, Code 6111, Naval Research Laboratory, Washington, D.C. 20375.

^{**} Present Address: Bruker Instruments, Inc., Manning Park, 19 Fortune Drive, Billerica, MA 01821.

Introduction

Clusters generated from III-V compound semiconductors have been the subject of recent studies involving theoretical modelling of the semiconductor surface,¹⁻³ the formation and photodissociation of positive heteroatomic Ga_xAs_y ions,^{4,5} the determination of electron affinities of negatively charged clusters⁶ and the electronic spectroscopy of neutral clusters.⁷ Quantitative analysis of trace impurities in semiconductors using laser ablation has become increasingly routine,^{8,9} and the generation of both hetero- and homoatomic clusters is often observed in these experiments.^{10,11} However, little is known about certain important physical properties, such as ionization potentials (IP's), of clusters from III-V materials and the charge transfer (CT) reactivities of ions produced from these materials have not been investigated. Better characterization of these properties should lead to a more complete understanding of their role in cluster generation, growth, and stability.

The clustering of laser evaporated atoms from both GaAs and InP semiconductors has been observed and studied.^{4-7,10,11} In experiments on the former material clusters of the general formula Ga_xAs_y were generated by vaporization using the second harmonic output of a Nd:YAG laser, entrained in helium carrier gas prior to supersonic expansion and, in positive ion studies, subsequently ionized by an excimer laser.^{4,6} Ga_xAs_y⁺ clusters up to x + y = 40 were generated. Negative ions consisting of both Ga_xAs_x⁻ and Ga_xAs_{2x}⁻ clusters up to x = 4 were also formed in related studies. Positively charged InP clusters have been produced in a similar manner.⁷ However, few homoatomic clusters were formed in these supersonic expansion studies. This is attributed to the nature of the supersonic expansion process, wherein small clusters are produced by direct vaporization but, by reaction with the large neutral population, have time to grow during their flight to the expansion orifice.¹² It is therefore quite likely that the cluster distribution from heteroatomic species formed in such a manner will not be the same as that formed by direct laser vaporization of a surface. This appears to be true; homoatomic phosphorus clusters up to P₄⁺ have been produced by direct laser vaporization of GaP without the formation of heteroatomic clusters.^{10,11}

Except for the production of As₄¹³ and P₄¹⁴⁻¹⁶ by thermal evaporation, formation of sufficient neutral populations of small As and P clusters for subsequent experimentation

has proven difficult. Most measurements to date have been made on heteroatomic clusters. Electron affinities of the heteroatomic GaAs clusters have been measured by photodetachment, either by monitoring the dependence of the ionization signal on the number of absorbed photons (and thus bracketing the electron attachment energy between that corresponding to an n and $n+1$ photon process), or by determining a threshold energy for photodetachment.⁶ Neutral electronic spectroscopy of InP clusters has recently been performed,⁷ but is only applicable for clusters which exhibit predissociation.

Information on the ionization potentials of clusters is not common, but can be obtained by chemical means via either charge transfer bracketing or equilibria experiments. In a Fourier transform ion cyclotron resonance (FTICR) mass spectrometer a specific cluster ion can be brought to near thermal energy by collisions with an appropriate gas, isolated, and allowed to react with charge transfer agents (CTA) of known IP. Ionization potentials can be determined to within ± 0.1 eV by observing the transition between no charge transfer, and charge transfer and rate coefficients also extracted by following the CT reaction as a function of time. This bracketing approach has proven valuable in the determination of carbon cluster IP's.¹⁷ In this paper the method has been extended to homoatomic arsenic and phosphorus clusters formed by laser desorption from GaAs and InP wafers, respectively.

Experimental

All experiments were performed on a home-built FTICR mass spectrometer equipped with a 2 Tesla superconducting magnet and a 2.54 cm cubic cell (see Figure 1), controlled by a Nicolet¹⁸ FTMS-1000 electronics console. This system has been customized to allow the introduction of laser light into any of three laser windows on the source side or two windows on the solids inlet flange. The vacuum chamber is pumped by two diffusion pumps¹⁹ of 300 and 700 L/sec pumping speed, respectively. This high pumping speed permits the thermalizing gas, which is introduced via a pulsed valve, to be pumped away rapidly so that pressures reach the 10^{-6} torr range during the FTICR detection phase. In all experiments ions with frequencies from 10 kHz to 2.667 MHz were excited and 25 to 50 time domain signals (depending on signal strength) containing 16



Distribution/	
Availability Codes	
Dist	Avail and/or Special
A-1	

K data points were averaged. The time domain signal was apodized using a modified Blackman-Harris window function²⁰ and zero-filled once prior to Fourier transformation. A 2 volt trapping potential was used; lower voltages resulted in decreased trapping efficiency.

The phosphorus and arsenic clusters were generated using a CO₂ laser²¹ operating in a pulsed mode (0.5 - 1 J/pulse, 1 μ s in duration). The output of this laser was focussed by a 7.6 cm focal length ZnSe lens (mounted inside the vacuum chamber near the ICR cell) through holes in both ICR cell trap plates onto a sample of InP or GaAs mounted on the end of a solids probe.²² The pulse energy of the CO₂ laser was adjusted to enhance the ion signal for an individual cluster ion. The samples were not rotated, as exposure of fresh vaporization sites did not enhance or alter the spectra.

The neutral reactants used for bracketing and their currently accepted IP's²³ are listed in Table 1. All chemicals were obtained commercially and used without further purification except for liquids, which were subjected to several freeze-pump-thaw cycles. The purity of each charge transfer agent was verified by acquiring wide mass range, electron ionization spectra. The CTA's were leaked into the vacuum chamber and their pressure maintained constant at a value between 2×10^{-6} and 5×10^{-7} torr above the background pressure. These pressures were generally kept as low as possible to minimize cluster ion loss due to reaction during the long thermalization period.

The pulse sequence employed has been thoroughly described.¹⁷ In brief, the firing of the CO₂ laser was followed closely (a few microseconds later) by the opening of a pulsed valve which released a burst of SF₆ or Ar. SF₆ was the preferred thermalizing gas, but Ar was used with several cluster ions which reacted with SF₆. The maximum pressure attained was 1.5×10^{-5} torr (uncorrected) as read on an ionization gauge. A series of ion ejections was then applied to isolate the desired reactant cluster ion. A one second delay then allowed sufficient time for many (ca. 150) thermalizing collisions between the selected cluster ion and the SF₆ or Ar neutral molecules, and also for the thermalizing gas to be pumped away. During the one second thermalization period formation of ion/molecule reaction products was often observed and it was therefore necessary to apply an additional set of ejection pulses identical to the first to remove them. Following the second set of ejection pulses the CT reaction of interest was monitored.

Reactions were typically followed to a maximum reaction time of 5 seconds, and complete mass spectra were obtained at 10 to 15 different reaction times in the range from ca. 50 ms to the maximum delay time studied. However, several reactions proceeded at very slow rates, and for them it was necessary to collect data for reaction times up to 20 s in duration. To compensate for fluctuations in total ion signal inherent in the laser desorption technique all peak intensities were normalized by dividing them by the sum of all peak intensities greater than 2% of the most intense peak. Reaction rates were extracted from the slope of the best linear fit of the natural log of the cluster ion intensity vs. reaction time. This approach is based upon the usual assumption that the ion/molecule reactions studied follow pseudo-first order kinetics. Pressures were corrected for differences in ionization gauge readings by calibration with a capacitance manometer. These corrected pressures were then multiplied by a system factor necessary to compensate for the difference in pressure as measured at the ionization gauge and at the FTICR cell location. The rate of the reaction $\text{CH}_4^+ + \text{CH}_4 \rightarrow \text{CH}_5^+ + \text{CH}_3$ was measured and comparison with known values²⁵ gave a system factor of 2.0.

Results

Arsenic cluster ions. A typical mass spectrum of the ions produced by CO₂ laser desorption from GaAs is shown in Figure 2a (with no ions ejected). Altering the laser pulse energy did not appreciably change the relative cluster distributions. Arsenic clusters up to n = 5 can be noted in the figure, but no heteroatomic Ga_xAs_y⁺ clusters were seen. In addition, the doubly charged ions ⁶⁹As²⁺, ⁷¹As²⁺ and As²⁺ are present. The intensity of the small As₅⁺ signal was still sufficient, after the ejection of higher intensity, lower mass clusters, to permit the CT reactions for this cluster to be monitored. Unfortunately the inconsistent nature of the As₅⁺ signal complicated efforts to extract rate coefficients for its reactions. Heteroatomic clusters were observed in the negative ion spectra, with Ga_xAs_y⁻ clusters up to x = 3, y = 2 and x = 2, y = 3 being formed. However, they were small in comparison to the large signal generated by As₂⁻ (see Figure 2b).

Table 2 summarizes the CTA's used to bracket each cluster's IP. The IP's reported in the upper half of Table 3 were taken as the midpoint of the gap between the IP's of neutrals for which charge transfer did and did not occur (cf. Tables 1 and 2). This

approach was straightforward for As_{3-6}^+ but more difficult for As^+ and As_2^+ , which quite often underwent reactions with the CTA's via pathways other than CT. Although these reactions hindered the IP bracketing they are interesting in their own right, and only the determination of the As ionization potential was negatively affected. Because As^+ reacted without charge transfer with 1,4-benzoquinone, its IP had to be bracketed between hexafluorobenzene and 1,2-dicyanobenzene (cf. Tables 1 and 2).

A representative plot of the normalized ion intensities vs. time for the reaction of As_4^+ with aniline is shown in Figure 3a. Plots similar to these were obtained for As^+ , As_2^+ and As_3^+ . Rate coefficients extracted from comparable data are listed in Table 4. When possible, rate coefficients for reactions with similar CTA's were measured so that direct comparisons of reaction rates could be made between cluster ions of varying size. During the course of these studies As^+ and As_2^+ were found to undergo numerous reactions other than charge transfer with some of the CTA's. The reaction product ions were typically fluorinated, oxygenated or acetylenated arsenic compounds. The major reactions observed are given in Table 5. Only ions are detected in the FTICR mass spectrometer, so the most stable possible neutral product of each reaction is given in the table.

Phosphorus cluster ions. The laser desorption mass spectrum of ions produced by 0.75 J/pulse irradiation of InP is shown in Figure 4a. At this laser pulse energy all ions have approximately equal intensities. However, the intensities of the phosphorus clusters were very dependent on the laser pulse energy and increasing or decreasing the laser pulse energy weighted the spectrum to lower or higher masses, respectively. At very low pulse energies predominantly P_3^+ and P_4^+ were formed as shown in Figure 4b (at 0.50 J/pulse). Turning the probe to expose a fresh ionization site did not affect the relative abundances, but the tightness of the focus did, in much the same manner as varying the laser pulse energy. No phosphorus clusters with more than 4 atoms, no mixed In_xP_y^+ clusters and no negative ions were observed.

The reactions of phosphorus clusters with the CTA's of Table 1 are summarized in the lower half of Table 2 and the ionization potentials determined are listed in the lower half of Table 3. Figure 3b shows a typical plot of P^+ ion intensity versus time as it reacts with C_2D_4 . The principle reaction sequence involves P^+ and C_2D_4 forming sequentially PC_2D_2^+ and then $\text{P}[\text{C}_2\text{D}_2]_2^+$. Table 4 (lower part) summarizes the rate coefficients

measured for P_n^+ CT reactions. As with arsenic, P^+ and P_2^+ proved to be extremely reactive and, similar to the arsenic case, the products of reactions other than CT were fluorinated, oxygenated or acetylenated neutrals or ions. These reactions are summarized in Table 5 (lower half).

Discussion

The determination of ionization potentials via the charge transfer bracketing technique is subject to several limitations which affect the precision of the method. The first is the spacing between the ionization potentials of neutrals which react with the cluster ions by charge transfer reactions. The problem is intensified by the tendency of small clusters to react with many CTA's via non-charge transfer reactions, thus further increasing the spacing between "suitable" CTA's. Furthermore, there are fewer reference compounds which can be used to determine the higher IP's of small cluster species (cf. Table 1). In this paper the cluster IP is reported as halfway between the IP of the compound of lowest IP for which charge transfer was not observed and the IP of the compound of highest IP for which it was observed. Since the IP of the cluster can lie anywhere in the gap between the two neutral IP's, the uncertainty stated is generally $\pm 1/2$ the gap size, or ± 0.1 eV when the $1/2$ of the gap was smaller than this amount.

Another source of error would be incomplete thermalization of the ions formed by laser desorption. We attempted to remove excess internal and translational energy via multiple collisions with a thermalizing gas. The clusters should then have been near thermal before their reactions with the CTA's were monitored, but if complete thermalization were not achieved the measured IP would be higher than the actual value. The As_n and P_n IP's determined in this work provide an indication of the validity of results obtained by charge transfer bracketing experiments, because values for at least the As and P ionization potentials have been determined previously by spectroscopic methods, and are thus known to high precision (and, hopefully, accuracy). The four previously-reported IP values (for As, P, P_2 , and P_4) judged most reliable by the authors of Ref. 23 lie near or just below the lower limits for the IP's determined by our charge transfer bracketing method. This suggests that some translational or internal energy remains in the cluster ions after the "thermalization" period. This point will be addressed more

completely in a subsequent publication.²⁸

Arsenic cluster ionization potentials. The cluster ion distribution produced by direct laser ablation of GaAs is notably different from that which results from MPI of supersonically expanded, laser vaporized GaAs (cf. Figure 2a and Figure 2 of Reference 6). As stated in the introduction this difference probably arises because of the opportunity for additional cluster formation before and during the expansion process. The cluster distribution shown here is more representative of the ion population which would be produced in laser analysis of semiconductor surfaces, where direct laser desorption is used.

The IP of As_2 is of particular interest. The value of 8.63 ± 0.10 eV reported here is 0.44 eV lower than the 9.07 ± 0.07 eV previously measured by observing the appearance potential of As_2^+ as a function of electron energy²⁷ (a value not considered firmly established)²³. The lack of charge transfer between As_2^+ and four different compounds whose IP's lie in the range 8.63 and 9.07 eV strongly supports the validity of the lower value reported here. Electron ionization is a vertical process,²⁸ and the lower CT value determined in this work suggests that the previously reported value is in error, or that the difference between the vertical and adiabatic IP's is substantial.

The currently quoted IP for As_2^+ was derived from the Rydberg series leading to the first IP and found to be 10.1 ± 0.2 eV.²⁹ Again, this value is not believed to firmly established.²³ The IP determined by charge transfer bracketing, 9.89 ± 0.10 eV (cf. Table 3), is lower than the previously reported value and is also less uncertain because of the small difference in IP's of the bracketing CTA's.

The IP for the atom As determined by CT was 10.00 ± 0.10 eV, slightly higher than the spectroscopically determined value of 9.7883 ± 0.0002 eV.²³ The large uncertainty in our value is due to the occurrence of an ion/molecule reaction between As^+ and 1,4-benzoquinone. However, As^+ did react via charge transfer with hexafluorobenzene (IP = 9.91 eV). AsF^+ and AsF_2^+ were also formed in this reaction, but there was no evidence of their subsequent reaction with neutral hexafluorobenzene to produce the observed C_6F_6^+ , whose formation was taken to indicate that the IP of As is greater than that of hexafluorobenzene. Any excess internal energy acquired by As^+ during the laser desorption process should be radiatively or collisionally quenched during the one second

thermalizing period and its translational energy should also be very near thermal after well over a hundred collisions.

The IP's for As_3 and As_5 have not been determined previously, primarily because of their absence in the vapor above heated arsenic. Both IP's were found to be several eV lower than those of the other arsenic clusters, with As_3 the lowest in this As_n series. A similar pattern was observed for the phosphorus clusters. An IP of 7.4 eV can be derived from the appearance potential of As_3^+ from As_4 ³⁰ and the heats of formation of As , As_3 , and As_4 .²³ This agrees well with the value of 7.46 ± 0.10 eV determined in this work by CT bracketing.

Phosphorus cluster ionization potentials. The molecule P_4 is the most studied of the phosphorus clusters. Bracketing between benzene and 1,2 difluorobenzene led to an IP of 9.28 ± 0.10 eV (CT also occurred with both fluorobenzene and m-dichlorobenzene). This value is slightly higher than that obtained in an early photoionization study¹³ (9.08 ± 0.05 eV), but is in good agreement with more recent work¹⁵ where the ionization onset was found at 9.25 eV. Our experiments also generated evidence that more than one isomer of P_4^+ is produced by laser vaporization. Figure 5 is a typical plot of reactant and product ions in the reaction between P_4^+ and benzene, and it is apparent that only approximately 40% of the P_4^+ ions react with benzene. Such incomplete reaction was seen regardless of the pressure of benzene or the reaction time. This implies that a percentage of the P_4^+ population has an IP lower than that of benzene but greater than that of fluorobenzene (IP = 9.25 eV), for which the CT always proceeded to completion.

The currently reported²³ value for the IP of P_3 (7.85 ± 0.2 eV) was not obtained directly, but rather was derived¹⁵ from the appearance potential of P_3^+ from P_4 and the dissociation energy of $\text{P}_4 \rightarrow \text{P}_3 + \text{P}$. The slightly higher value reported here, 8.09 ± 0.10 eV, is more precise. The IP of P_2 determined by CT is 10.6 ± 0.1 eV which agrees with the 10.53 eV derived by Huber and Herzberg.³¹ The coupling of laser desorption and CT bracketing allows for the direct determination of these IP's which are difficult to study by other methods. The P atom was found by CT bracketing to have an IP of 10.50 ± 0.10 eV, in good agreement with the previously reported 10.486 eV.³²

Rate coefficients. Charge transfer reactions which occur via an ion-induced dipole orbiting "Langevin"³³ collision should be adiabatic, with equilibration to the lowest energy

product species before separation. However, the majority of ionization potentials are measured by vertical processes (such as photoionization). The difference between the adiabatic and vertical IP's will be determined by the overlap between the neutral and ion potential surfaces and the depths of the respective potential minima. This difference can be on the order of 0.1 - 0.7 eV.³⁴

In order to ensure that the CT reaction is an adiabatic process it should proceed no faster than the Langevin³³ rate limit. A faster rate than this indicates a long range electron jump mechanism in which an ion/molecule complex does not form, which may lead to a vertical rather than adiabatic IP. The rate coefficients measured and reported in Table 4 are all at or less than the Langevin rate limit (not every collision results in a reaction). Of a total of four CT reactions studied with and without thermalizing gas, all but one rate constant showed little or no dependence on the additive of the thermalizing gas. This is not surprising as CT reactions with rate coefficients near the Langevin rate limit are typically not temperature dependent.³⁵

One reaction which proceeded at a much slower rate than the others, $\text{As}_4^+ + m\text{-C}_6\text{H}_4(\text{CH}_3)_2 \rightarrow \text{As}_4 + m\text{-C}_6\text{H}_4(\text{CH}_3)_2^+$, showed a noticeable change in rate coefficients when a thermalizing gas was introduced. In the absence of thermalizing gas (i.e. when the ions probably possessed greater amounts of internal and translational energy) was approximately 75% slower than it was when As_4^+ was thermalized prior to reaction. This may be due to a reaction in which competition exists in the ion/molecule complex between CT and back reaction to form the original reactants. The exothermic CT route is therefore favored at lower temperatures.³⁵ Although the excess internal energy present without thermalization did not adversely effect the IP bracketing, this does demonstrate that the thermalizing gas is necessary to remove excess energy in these CT reactions if a thermal rate constant is to be extracted, especially if the rate coefficients are small.

*Novel reaction pathways.*³⁶ The extreme reactivity of As^+ , As_2^+ , P^+ and P_2^+ with the CTA's provided the opportunity to observe several unusual reactions. The larger clusters investigated were not as reactive as these four smaller ions. In fact, the only reactions other than charge transfer of the five larger cluster ions involved the formation of the adducts aniline- P_3^+ , *m*-toluidine- As_3^+ and azulene- As_3^+ . Thus the following discussion is limited to As_n^+ and P_n^+ , where $n = 1$ or 2 .

Upper limits on heats of formation for a few species produced in the observed ion/molecule reactions have been derived (ΔH , values calculated in this manner are in italics) by assuming the observed reaction to be thermoneutral or exothermic and employing known ΔH , values for the reactants and one of the product species.²³ If the reaction is significantly exothermic, the derived value is likely to be considerably higher than the actual value, but at least an upper limit can be stated. All reactions referenced are catalogued in Table 5.

Reactivity of As^+ , As_2^+ , P^+ , and P_2^+ (reactions 1, 9, 14 and 21 respectively) with SF_6 forced the use of Ar as the thermalizing gas for all four ions. This leads to an upper limit for the ΔH , of AsF , As_2F and P_2F of 225, 205 and 205 kcal/mol, respectively, although these limits are probably quite high (for comparison the ΔH , of PF is -12.5 kcal/mol²³). When reacting with H_2O , all four ionic species formed oxides (reactions 2, 10, 15, 22). Side reactions of this type make it imperative that low background pressures (water is the prime component of the background in our instrument) and anhydrous CTA's be used in the CT bracketing experiments.

Several ions and neutrals were formed repeatedly in a number of the ion/molecule reactions. As demonstrated in the reactions with SF_6 and H_2O , fluorination and oxygenation result when the small clusters react with CTA's which can provide fluorine or oxygen atoms: fluorinated benzenes, nitrobenzenes and quinones (reactions 7, 8, 12, 13, 19, 20, 25). Of the product ions and neutrals, only the ΔH 's for PO^+ (186 kcal/mol), PO (-8 kcal/mol), and PF (-12.5 kcal/mol) have previously been measured.²³ The driving force behind the above reactions appears to be the high ΔH 's of the laser desorbed species: $As^+ = 298$ kcal/mol, $As_2^+ = 278$ kcal/mol, $P^+ = 317$ kcal/mol and $P_2^+ = 277$ kcal/mol.²³ For example, the reaction $P^+ + H_2O \rightarrow PO^+ + H_2$ has a ΔH of -73 kcal/mol and for the reaction $As^+ + H_2O \rightarrow AsO^+ + H_2$ the ΔH , of AsO^+ only needs to be ≤ 240 kcal/mol for an exothermic reaction to occur. Given these numbers it is evident why these ionic species are so reactive. The arsenic ions were also able to extract a second fluorine or oxygen to form AsF_2^+ and $As_2O_2^+$ (reactions 8b, 13b).

Perhaps the most intriguing reactions were those with ethylene, acetylene and other compounds which could provide C_2H_2 groups (reactions 3, 5, 6, 16, 17, 23, 24). As^+ and P^+ reacted with ethylene to form $AsC_2H_2^+$ (ΔH , ≤ 310 kcal/mol) and $PC_2H_2^+$ (ΔH , ≤ 319

kcal/mol), which reacted further to produce $\text{As}[\text{C}_2\text{H}_2]_2^+$ and $\text{P}[\text{C}_2\text{H}_2]_2^+$. These reactions are unusual in that it appears a complex is being formed between acetylene and the As^+ or P^+ ion. Similar dehydrogenation reactions have been reported for bare transition metals ions³⁷. In addition, reactions of As^+ with quinone and 1,4-naphthoquinone (reactions 5,6) produced AsC_2H_2^+ and $\text{As}[\text{C}_2\text{H}_2]_2^+$, however the reaction of quinone with As_2^+ (reaction 13) formed As_2O^+ and As_2O_2^+ instead. As_2^+ did not react with ethylene but P_2^+ (reaction 23) formed P_2CH^+ ($\Delta H, \leq 255$ kcal/mol). As^+ did not react with acetylene, although P^+ did (reaction 17). However, formation of PC_2H_2^+ , which might have been expected, was not observed. Instead PC_2H^+ ($\Delta H, \leq 320$ kcal/mol) and subsequently $\text{P}[\text{C}_2\text{H}]_2^+$ were formed, with the elimination of H atoms. Interestingly, it was possible to create PC_2H_2^+ (reaction 24), but only via the reaction of P_2^+ with acetylene (a P atom is eliminated). This now places an upper limit on the ΔH of PC_2H_2^+ of 256 kcal/mol. The reaction of benzene and P^+ (reaction 18) also produces interesting products: C_5H_5^+ (HCP eliminated) and PC_4H_4^+ ($\Delta H, \leq 280$ kcal/mol).

Conclusions

The determination of ionization potentials using charge transfer reactions has proven valuable for phosphorus and arsenic clusters formed by direct laser vaporization. The IP's for As_2 , As_4 , P_3 , and P_4 have been determined with less uncertainty than that reported earlier, and the previously undetermined IP's for As_3 and As_5 have been ascertained. The CT IP of atomic P agree well with that determined by accurate spectroscopic methods, adding credibility to the technique.

The validity of measuring IP's using charge transfer techniques has been strengthened by carefully studying rate coefficients of the reactions involved. These rate coefficients were found to be near or slower than the Langevin rate limit, indicating that CT occurred through a long-lived collision, presumably resulting in adiabatic IP's. For As_4^+ the difference between vertical and adiabatic IP's has been shown to be significant, assuming that the previously measured value is accurate.

Quenching of the translational and internal energy through neutral gas collisions has been shown to affect the rate of at least one reaction. However there was no evidence that the IP's would have been inflated in the absence of the thermalizing gas.

Non-CT reactions provided new insight into the reactivity of P^+ , P_2^+ , As^+ and As_2^+ . The consecutive addition of C_2H_2 groups to P^+ , As^+ and As_2^+ from quinones or by the dehydrogenation of ethylene are perhaps the most interesting of these reactions, and are similar to dehydrogenation observed in transition metal chemistry.

Acknowledgements

This work was supported in part by the Office of Naval Research. We thank Dr. K. R. Williams for numerous helpful comments and Dr. T. J. Anderson for providing the InP and GaAs samples.

References

- (1) Pearson, E.; Halicioglu, T.; Tiller, W.A. *Surf. Sci.* **1987**, *184*, 401.
- (2) Choi, D.K.; Koch, S.M.; Halicioglu, T.; Tiller, W.A. *J. Vac. Sci. Technol. B* **1988**, *6*(4), 1140.
- (3) Delerue, C.; Lannoo, M.; Allan, G. *Phys. Rev. B* **1989**, *39*, 1669.
- (4) O'Brian, S.C.; Liu, Q.Z.; Heath, J.R.; Tittel, F.K.; Curl, R.F.; Smalley, R.E. *J. Chem. Phys.* **1986**, *84*(7), 4074.
- (5) Zhang, Q.-L.; Lui, Y.; Curl, R.F.; Tittle, F.K.; Smalley, R.E. *J. Chem. Phys.* **1988**, *88*(3), 1670.
- (6) Lui, Y.; Zhang, Q.-L.; Tittle, F.K.; Curl, R.F.; Smalley, R.E. *J. Chem. Phys.* **1986**, *85*(12), 7434.
- (7) Kolenbrander, K.D.; Mandich, M.L. *J. Chem. Phys.* **1989**, *90*(10), 5884.
- (8) Parks, J.E.; Spaar, M.T.; Cressman, P.J. *J. Crystal Growth* **1988**, *89*, 4.
- (9) Schueler, B.; Odom, R.W. *J. Appl. Phys.* **1987**, *61*(9), 4652.
- (10) Namiki, A.; Seiji, C.; Ichige, K. *Jpn. J. Appl. Phys.* **1987**, *26*(1), 39.
- (11) Tomita, M.; Kuroda, T. *Surf. Sci.* **1988**, *201*, 385.
- (12) Smalley, R.E. *Anal. Instru.* **1988**, *17*(1&2), 1.
- (13) Hart, R.R.; Robin, M.B.; Kuebler, N.A. *J. Chem. Phys.* **1964**, *42*(10), 3631.
- (14) Bennett, S.L.; Margrave, J.L.; Franklin, J.L. *J. Chem. Phys.* **1974**, *61*(5), 1647.
- (15) Smets, J.; Coppens, P.; Drowart, J. *J. Chem. Phys.* **1977**, *20*, 243.
- (16) Bennett, S.L.; Margrave, J.L.; Franklin, J.L.; Hudson, J.E. *J. Chem. Phys.* **1973**, *59*(11), 5814.
- (17) Bach, S.B.H.; Eyler, J.R. *J. Chem. Phys.* **1990**, *92*, 358.
- (18) Now sold by Extrel, P.O. Box 4508, Madison, WI 53711, U.S.A.
- (19) Alcatel Vacuum Products, 40 Pondpark Road, Hingham, MA 02043, U.S.A.
- (20) Harris, F.J. *Proc. IEEE* **1987**, *66*, 51.

(21) Lumonics Model 860-4 excimer laser, 105 Schneider Road, Kanata, ON K2K 1Y3 Canada, modified with IR optics and using a static CO₂ gas mixture.

(22) The GaAs and InP samples were mounted on the end of the solids probe shown in Figure 2 of Watson, C.H.; Baykut, G.; Eyler, J.R. *Anal. Chem.* **1987**, *59*, 1133.

(23) Lias, S.G.; Bartmess, J.E.; Liebman, J.F.; Holmes, J.L.; Levin, R.D.; Mallard, W.G. *J. Phys. Chem. Ref. Data* **1988**, *Suppl. No. 1*.

(24) General Valve Corp. Model 9-181-900, 202 Fairfield Rd., P.O. Box 1333, Fairfield, NJ 07006.

(25) An average rate coefficient of $1.13 \times 10^{-6} \text{ cm}^3 \text{ s}^{-1}$ compiled from Ikezoe, Y.; Matsuoko, S.; Takebo, M.; Viggiano, A. *Gas Phase Ion-Molecule Reaction Rate Constants Through 1986*; Maruzen Co., Ltd.: Tokyo, 1987.

(26) Zimmerman, J.A.; Bach, S.B.H.; Eyler, J.R. in preparation.

(27) Westmore, J.B.; Mann, K.H.; Tickner, A.W. *J. Phys. Chem.* **1964**, *68*, 606.

(28) Williams, D.H.; Howe, I. *Principles of Organic Mass Spectrometry*; McGraw-Hill Book Company (UK) Limited: London, 1972; Chapter 2.

(29) Donovan, R.J.; Strachan, P. *Trans. Faraday Soc.* **1971**, *67*, 3407.

(30) Hirayama, C.; Straw, R.D.; Hobgood, H.M. *J. of the Less-Common Metals* **1985**, *109*, 331.

(31) a) Huber, K.P.; Herzberg, G. *Molecular Spectra and Molecular Structure. IV. Constants of Diatomic Molecules*; Van Nostrand Reinhold Co.: Amsterdam, 1979; 518. Photoelectron spectrum used to determine IP was obtained from Bulgin, D.K.; Dyke, J.M.; Morris, A. *J. Chem. Soc. Faraday Trans. II* **1976**, *72*, 2225.

(32) Moore, C.E. *Ionization Potentials and Ionization Limits Derived from the Analyses of Optical Spectra*; Natl. Stand. Ref. Data Ser.: Natl. Bur. Stand. NSRDS-NBS 34 1970.

(33) Langevin, P.M. *Ann. Chim. Phys.* **1905**, *5*, 245. Translated in McDaniel, E.W. *Collision Phenomena in Ionized Gases*; John Wiley and Sons: New York, 1964, Appendix II.

(34) Lossing, F.P.; *Can. J. Chem.* **1971**, *49*, 357.

(35) Meot-Ner (Mautner), M. *Gas Phase Ion Chemistry, Volume 1*; Bowers, M.T., Eds.; Academic Press: New York, 1979, Chapter 6.

(36) All ΔH, used in this section were obtained from Reference 23.

(37) For a review see: Allison, J. *Prog. Inorg. Chem.* **1986**, *34*, 627.

Table 1. Charge Transfer Agents Used in this Study.

IP ²³ (eV)	Compound
6.83	N,N-diethyl-p-toluidine
6.93	N,N-dimethyl-p-toluidine
7.00	N,N-diethylaniline
7.13	N,N-dimethylaniline
7.41	azulene
7.50	m-toluidine
7.72	aniline
7.78	phenyl-1,4-benzoquinone
7.80	2-naphthol
7.85	hexamethylbenzene
8.04	durene
8.13	p-cresol
8.29	m-cresol
8.44	p-xylene
8.56	m-xylene
8.69	p-chlorotoluene
8.82	toluene
8.89	p-dichlorobenzene
9.04	1,2,4-trichlorobenzene
9.11	m-dichlorobenzene
9.18	1,4-difluorobenzene
9.20	fluorobenzene
9.25	benzene
9.30	1,2-difluorobenzene
9.32	tetrachloroethylene
9.35	1,3-difluorobenzene
9.45	2-nitrotoluene
9.48	3-nitrotoluene
9.56	1,4-naphthoquinone
9.88	1-fluoro-3-nitrobenzene
9.91	hexafluorobenzene
10.04	1,4-benzoquinone
10.10	1,2-dicyanobenzene
10.10	1,4-dicyanobenzene
10.23	4-nitrobenzonitrile
10.29	3-nitrobenzonitrile
10.30	1,4-dinitrobenzene
10.43	1,3-dinitrobenzene
10.507	ethylene
10.528	ethylene-d,
10.57	hexafluoro-m-xylene

Table 1 continues on next page.

Table 1, cont.

10.7	tetrafluoro-1,4-benzoquinone
11.18	difluoroacetylene
11.394	acetylene
11.77	tetracyanoethylene
12.130	xenon
12.194	acetonitrile
13.997	krypton

Table 2. Charge Transfer Agents whose IP's Bracketed Those of the As and P Clusters.

Cluster	CTA (charge transfer, no charge transfer)
As	hexafluorobenzene, 1,2-dicyanobenzene
As ₂	1-fluoro-3-nitrobenzene, hexafluorobenzene
As ₃	azulene, m-toluidine
As ₄	m-xylene, p-chlorotoluene
As ₅	hexamethylbenzene, durene
P	1,3-dinitrobenzene, hexafluoro-m-xylene
P ₂	hexafluoro-m-xylene, tetrafluoro-1,4-benzoquinone
P ₃	durene, p-cresol
P ₄	benzene, 1,2-difluorobenzene

Table 3. Ionization Potentials Determined by Charge Transfer Bracketing (eV).

Species	This work	Literature*
As	10.00 \pm 0.10	9.7883
As ₂	9.89 \pm 0.10	(10.1 \pm 0.2)
As ₃	7.46 \pm 0.10	NA
As ₄	8.63 \pm 0.10	(9.07 \pm 0.07)
As ₅	7.95 \pm 0.10	NA
P	10.50 \pm 0.10	10.486
P ₂	10.6 \pm 0.1	10.53
P ₃	8.09 \pm 0.10	(7.85 \pm 0.2)
P ₄	9.28 \pm 0.10 ^{**}	9.08 \pm 0.05
	9.23 \pm 0.10 ^{**}	

* Values in parentheses are those which are "considered not to be firmly established"²³ and contain a higher degree of uncertainty.

** Two isomeric forms of P₄ are present, see text.

Table 4. Rate coefficients of Arsenic and Phosphorus Cluster Ion Reactions.

Reactants	Rate Coefficient ($10^{-10} \text{ cm}^3 \text{ s}^{-1}$)
As ⁺ , ethylene	7.2 \pm 1.4
As ⁺ , ethylene-d ₄	6.4 \pm 1.3
As ⁺ , benzene	9.8 \pm 2.0
As ⁺ , toluene	7.4 \pm 1.5
As ⁺ , hexafluorobenzene	3.4 \pm 0.7
As ₂ ⁺ , benzene	6.4 \pm 1.3
As ₂ ⁺ , toluene	6.3 \pm 1.3
As ₂ ⁺ , 1-fluoronitrobenzene	2.6 \pm 0.5
As ₃ ⁺ , azulene	2.0 \pm 0.4
As ₃ ⁺ , dimethyltoluidine	3.9 \pm 0.8
As ₄ ⁺ , durene	5.4 \pm 1.1
As ₄ ⁺ , hexamethylbenzene	12.9 \pm 2.6
As ₄ ⁺ , aniline	4.1 \pm 0.8
As ₄ ⁺ , azulene	3.2 \pm 0.6
As ₄ ⁺ , m-xylene (no SF ₆)	0.35 \pm 0.07
As ₄ ⁺ , m-xylene (with SF ₆)	0.47 \pm 0.09
P ⁺ , ethylene	13.1 \pm 2.6
P ⁺ , ethylene-d ₄	9.5 \pm 1.9
P ⁺ , benzene	8.2 \pm 1.6
P ₂ ⁺ , ethylene	8.9 \pm 1.8
P ₂ ⁺ , ethylene-d ₄	7.4 \pm 1.5
P ₂ ⁺ , benzene	7.7 \pm 1.5
P ₃ ⁺ , durene	6.7 \pm 1.3
P ₃ ⁺ , hexamethylbenzene	10.5 \pm 2.1
P ₃ ⁺ , aniline	1.2 \pm 0.2
P ₄ ⁺ , durene	5.6 \pm 1.1
P ₄ ⁺ , hexamethylbenzene	12.4 \pm 2.5
P ₄ ⁺ , aniline	2.3 \pm 0.5
P ₄ ⁺ , m-dichlorobenzene	2.5 \pm 0.5
P ₄ ⁺ , benzene	2.8 \pm 0.6 [*]

* This reaction does not go to completion, see text.

Table 5. Reactions of Phosphorus and Arsenic Ions with Various CTA's.*

(1) $\text{As}^+ + \text{SF}_6 \rightarrow \text{SF}_5^+ + \text{AsF}$
 (2) $\text{As}^+ + \text{H}_2\text{O} \rightarrow \text{AsO}^+ + \text{H}_2$
 (3a) $\text{As}^+ + \text{C}_2\text{H}_4 \rightarrow \text{AsC}_2\text{H}_2^+ + \text{H}_2$
 (3b) $\text{AsC}_2\text{H}_2^+ + \text{C}_2\text{H}_4 \rightarrow \text{As}[\text{C}_2\text{H}_2]_2^+ + \text{H}_2$
 (4) $\text{As}^+ + \text{C}_2\text{H}_2 \rightarrow \text{NR}$
 (5a) $\text{As}^+ + \text{C}_{10}\text{H}_8\text{O}_2$ (1,4-naphthoquinone) $\rightarrow \text{AsC}_2\text{H}_2^+ + \text{C}_8\text{H}_4\text{O}_2$
 (5b) $\text{AsC}_2\text{H}_2^+ + \text{C}_{10}\text{H}_8\text{O}_2$ (1,4-naphthoquinone) $\rightarrow \text{As}[\text{C}_2\text{H}_2]_2^+ + \text{C}_8\text{H}_4\text{O}_2$
 (6a) $\text{As}^+ + \text{C}_6\text{H}_4\text{O}_2$ (quinone) $\rightarrow \text{AsC}_2\text{H}_2^+ + \text{C}_4\text{H}_2\text{O}_2$
 (6b) $\text{AsC}_2\text{H}_2^+ + \text{C}_6\text{H}_4\text{O}_2$ (quinone) $\rightarrow \text{As}[\text{C}_2\text{H}_2]_2^+ + \text{C}_4\text{H}_2\text{O}_2$
 (7a) $\text{As}^+ + \text{C}_6\text{H}_4\text{FNO}_2$ (1-fluoro-3-nitrobenzene) $\rightarrow \text{AsO}^+ + \text{C}_6\text{H}_4\text{FNO}$
 (7b) $\text{As}^+ + \text{C}_6\text{H}_4\text{FNO}_2$ (1-fluoro-3-nitrobenzene) $\rightarrow \text{C}_6\text{H}_4\text{FNO}^+ + \text{AsO}$
 (8a) $\text{As}^+ + \text{C}_6\text{F}_6$ (hexafluorobenzene) $\rightarrow \text{AsF}^+ + \text{C}_6\text{F}_5$
 (8b) $\text{AsF}^+ + \text{C}_6\text{F}_6$ (hexafluorobenzene) $\rightarrow \text{AsF}_2^+ + \text{C}_6\text{F}_5$

 (9) $\text{As}_2^+ + \text{SF}_6 \rightarrow \text{SF}_5^+ + \text{As}_2\text{F}$
 (10) $\text{As}_2^+ + \text{H}_2\text{O} \rightarrow \text{As}_2\text{O}^+ + \text{H}_2$
 (11) $\text{As}_2^+ + \text{C}_2\text{H}_4 \rightarrow \text{NR}$
 (12a) $\text{As}_2^+ + \text{C}_6\text{H}_4\text{FNO}_2$ (1-fluoro-3-nitrobenzene) $\rightarrow \text{C}_6\text{H}_4\text{FNO}^+ + \text{As}_2\text{O}$
 (12b) $\text{As}_2^+ + \text{C}_6\text{H}_4\text{FNO}_2$ (1-fluoro-3-nitrobenzene) $\rightarrow \text{As}_2\text{O}^+ + \text{C}_6\text{H}_4\text{FNO}$
 (13a) $\text{As}_2^+ + \text{C}_6\text{H}_4\text{O}_2$ (quinone) $\rightarrow \text{As}_2\text{O}^+ + \text{C}_6\text{H}_4\text{O}$
 (13b) $\text{As}_2\text{O}^+ + \text{C}_6\text{H}_4\text{O}_2$ (quinone) $\rightarrow \text{As}_2\text{O}_2^+ + \text{C}_6\text{H}_4\text{O}$

 (14) $\text{P}^+ + \text{SF}_6 \rightarrow \text{SF}_5^+ + \text{PF}$
 (15) $\text{P}^+ + \text{H}_2\text{O} \rightarrow \text{PO}^+ + \text{H}_2$
 (16a) $\text{P}^+ + \text{C}_2\text{H}_4 \rightarrow \text{PC}_2\text{H}_2^+ + \text{H}_2$
 (16b) $\text{PC}_2\text{H}_2^+ + \text{C}_2\text{H}_4 \rightarrow \text{P}[\text{C}_2\text{H}_2]_2^+ + \text{H}_2$
 (17a) $\text{P}^+ + \text{C}_2\text{H}_2 \rightarrow \text{PC}_2\text{H}^+ + \text{H}$
 (17b) $\text{PC}_2\text{H}^+ + \text{C}_2\text{H}_2 \rightarrow \text{P}[\text{C}_2\text{H}]_2^+ + \text{H}$
 (18a) $\text{P}^+ + \text{C}_6\text{H}_6$ (benzene) $\rightarrow \text{C}_6\text{H}_5^+ + \text{HCP}$
 (18b) $\text{P}^+ + \text{C}_6\text{H}_6$ (benzene) $\rightarrow \text{PC}_4\text{H}_4^+ + \text{C}_2\text{H}_2$

Table 5 continues on the next page.

Table 5, cont.

(19) $P^+ + m\text{-C}_6\text{H}_4(\text{CF}_3)_2$ (m-hexafluoroxylene) $\rightarrow \text{C}_6\text{H}_4\text{CF}_3\text{CF}_2^+ + \text{PF}$

(20) $P^+ + \text{C}_6\text{H}_4(\text{NO}_2)_2$ (1,2-dinitrobenzene) $\rightarrow \text{C}_6\text{H}_4\text{NO}_2\text{NO}^+ + \text{PO}$

(21) $P_2^+ + \text{SF}_6 \rightarrow \text{SF}_5^+ + \text{P}_2\text{F}$

(22) $P_2^+ + \text{H}_2\text{O} \rightarrow \text{P}_2\text{O}^+ + \text{H}_2$

(23) $P_2^+ + \text{C}_2\text{H}_4 \rightarrow \text{P}_2\text{CH}^+ + \text{CH}_3$

(24) $P_2^+ + \text{C}_2\text{H}_2 \rightarrow \text{PC}_2\text{H}_2^+ + \text{P}$

(25) $P_2^+ + \text{C}_6\text{H}_4(\text{NO}_2)_2$ (1,2-dinitrobenzene) $\rightarrow \text{C}_6\text{H}_4\text{NO}_2\text{NO}^+ + \text{P}_2\text{O}$

* The most stable neutral product is shown.

Figure Captions:

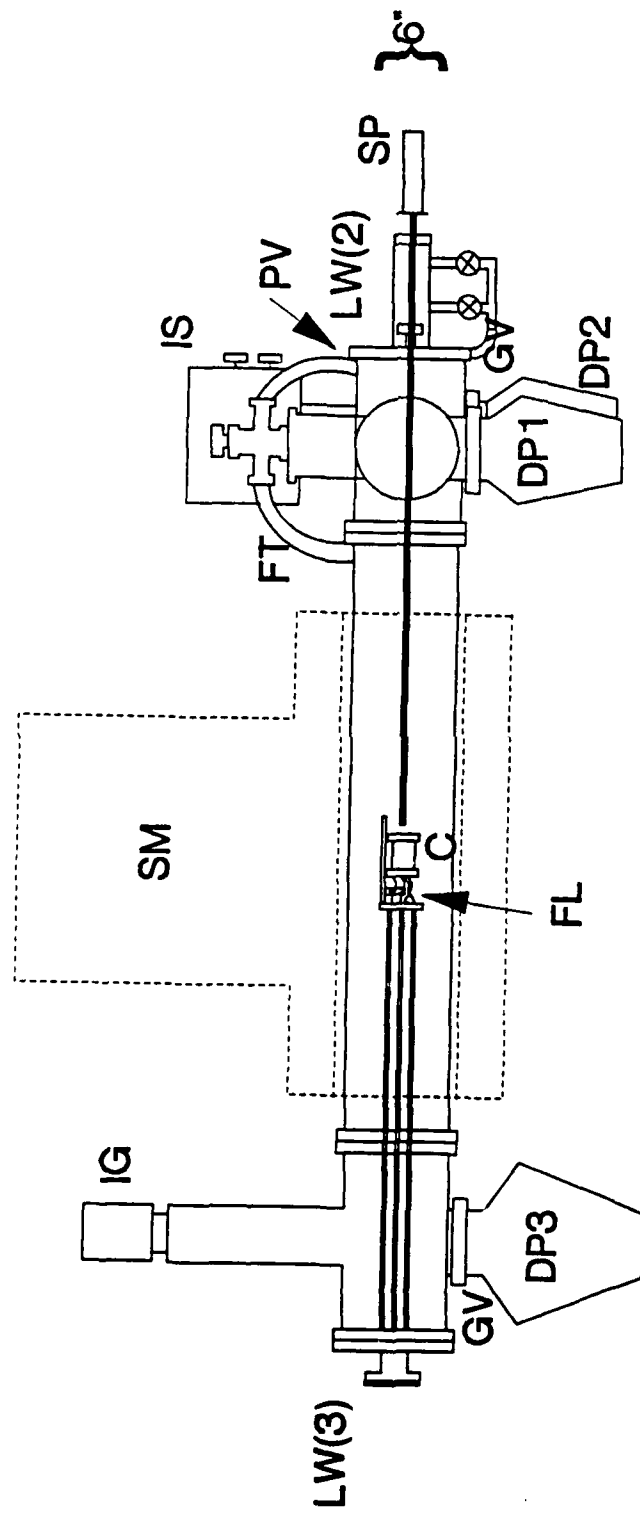
Figure 1. Diagram of the customized FTICR system. SM = 2 Tesla superconducting magnet, IS = inlet system, IG = ionization gauge, GV = gate valve, SP = solids probe, PV = pulsed valves, FT = flexible tubing to the pulsed valve vacuum transfer line, DP1 = inlet diffusion pump (300 L/s), DP2 = vacuum chamber diffusion pump (300 L/s), DP3 = vacuum chamber diffusion pump (700 L/s), LW(2) = flange with two laser windows, LW(3) = flange with three laser windows, FL = 7.6 cm focal length lens and C = 2.54 cm cubic ICR cell.

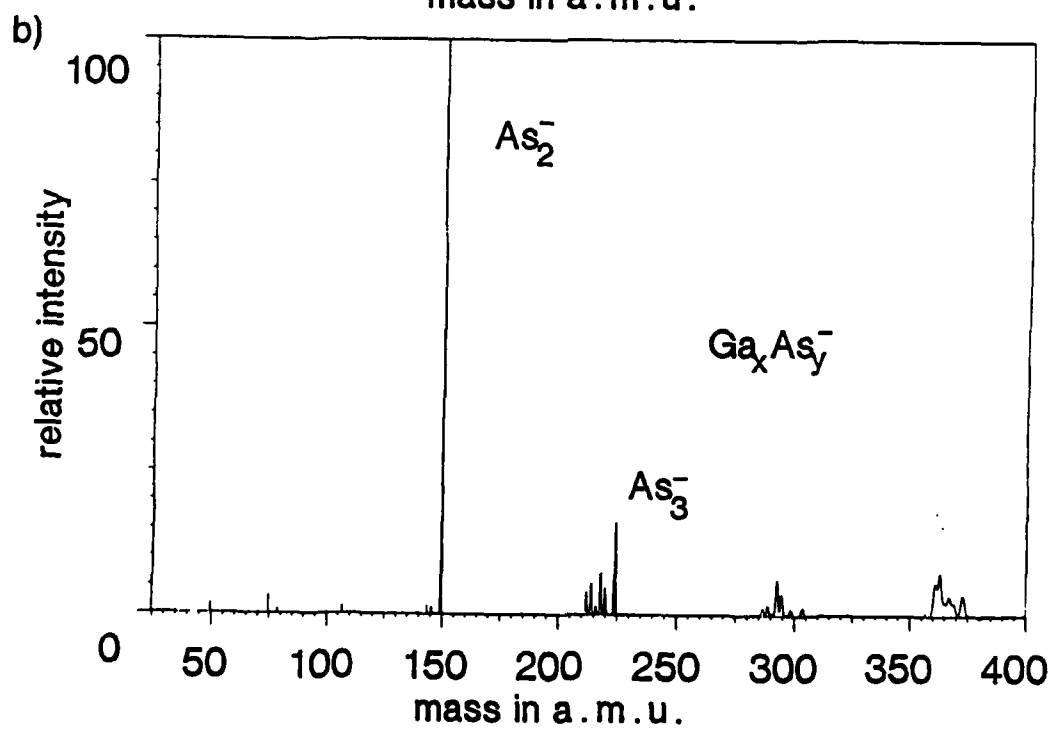
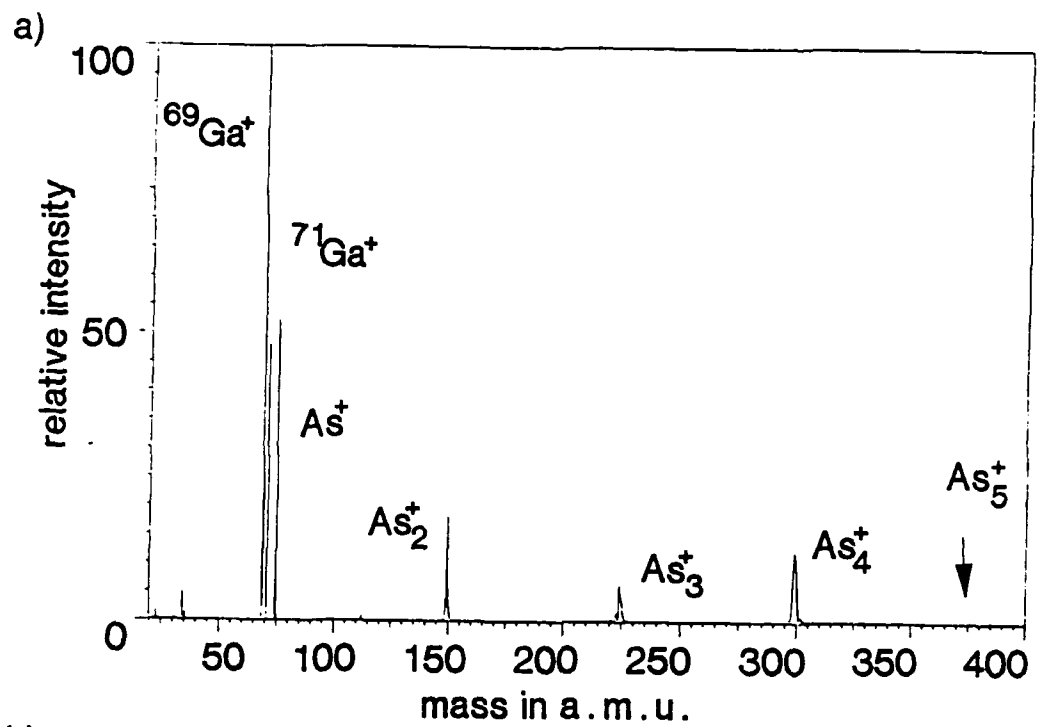
Figure 2. (a) Mass spectrum of positive ions produced by pulsed CO₂ laser irradiation of GaAs. (b) Mass spectrum of negative ions produced by pulsed CO₂ laser irradiation of GaAs. Heteroatomic Ga_xAs_y⁻ where x = 2,3 and y = 1,2,3 are formed.

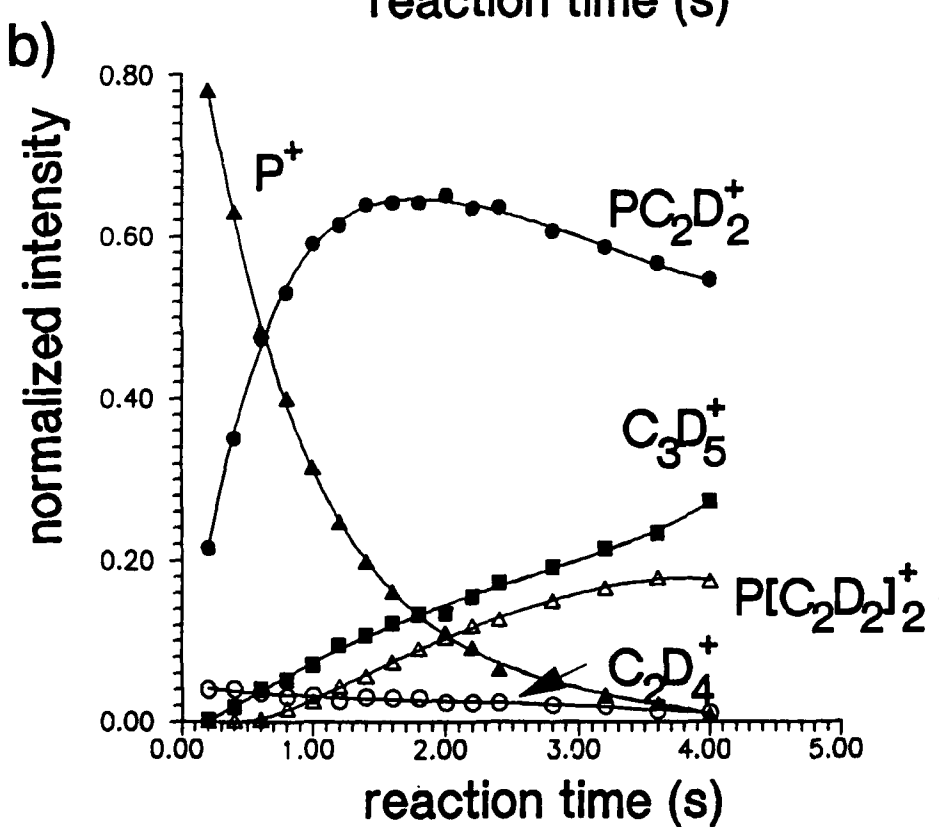
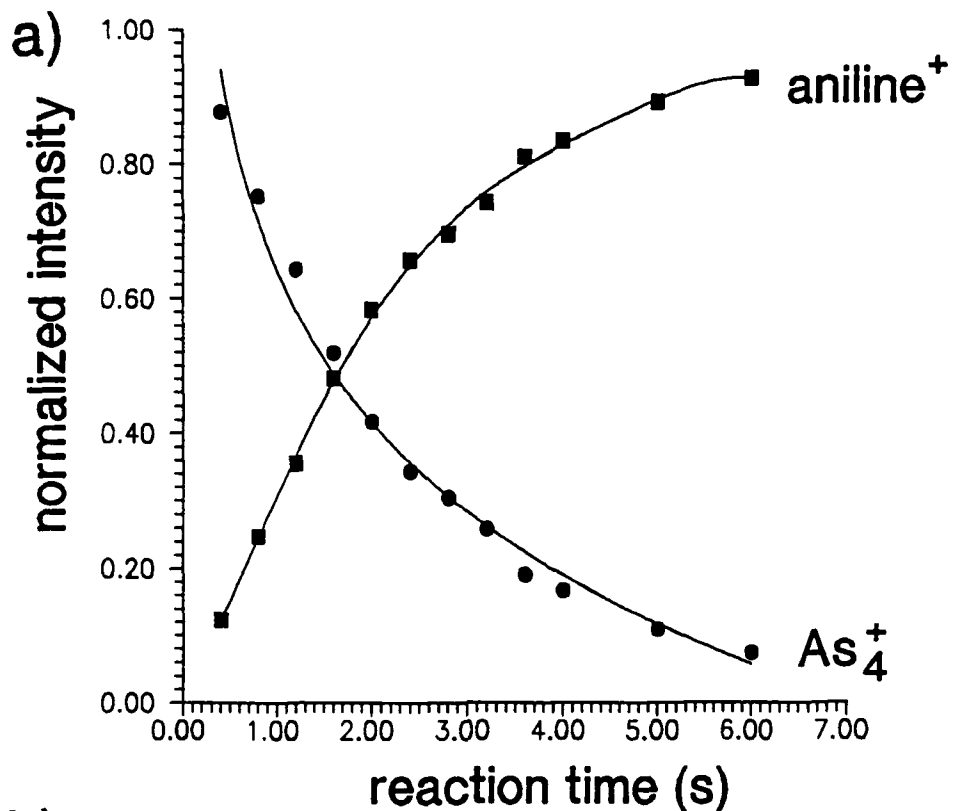
Figure 3. (a) Normalized ion intensities of As₄⁺ and C₆H₅NH₂⁺ vs. reaction time for the reaction As₄⁺ + C₆H₅NH₂ → As₄ + C₆H₅NH₂⁺. (b) Normalized ion intensities for P⁺, PC₂D₂⁺, P[C₂D₂]₂⁺, C₃D₅⁺ and C₂D₄⁺ vs. reaction time.

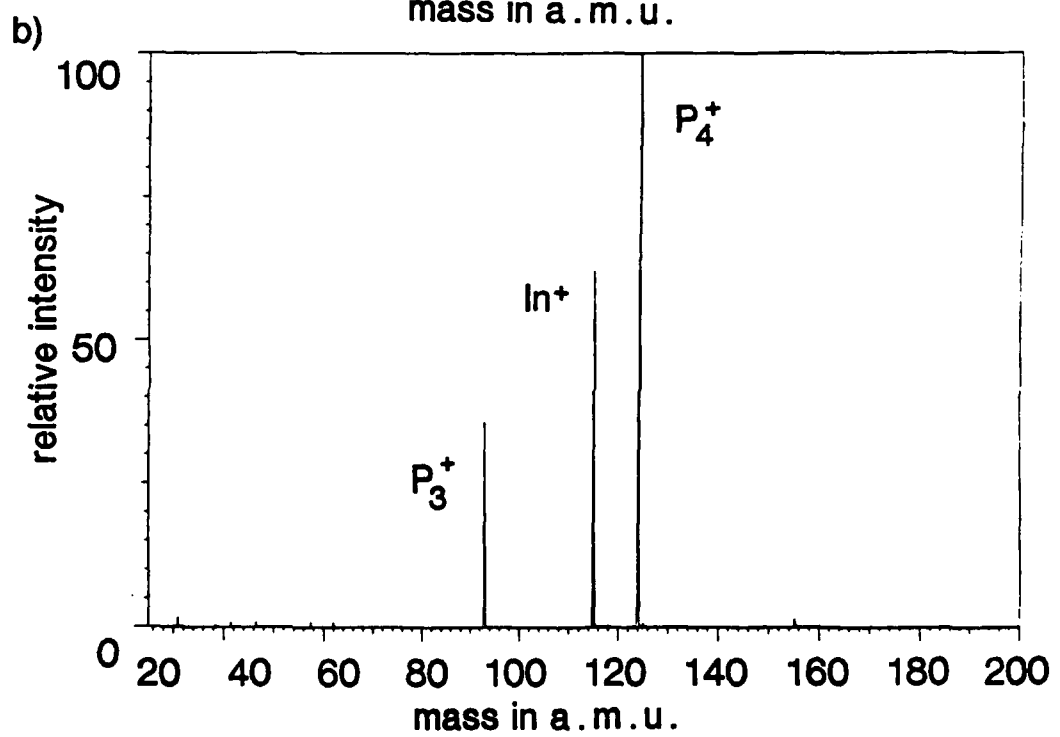
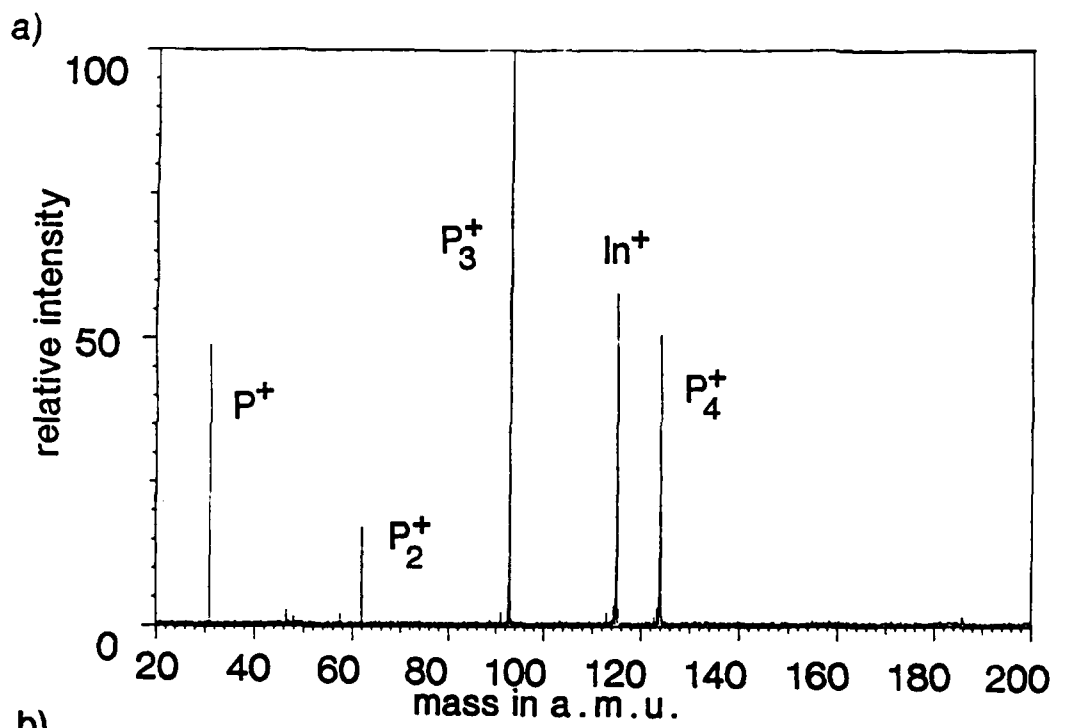
Figure 4. Mass spectra of positive ions produced by pulsed CO₂ laser irradiation of InP. (a) 0.75 J/pulse; (b) 0.50 J/pulse.

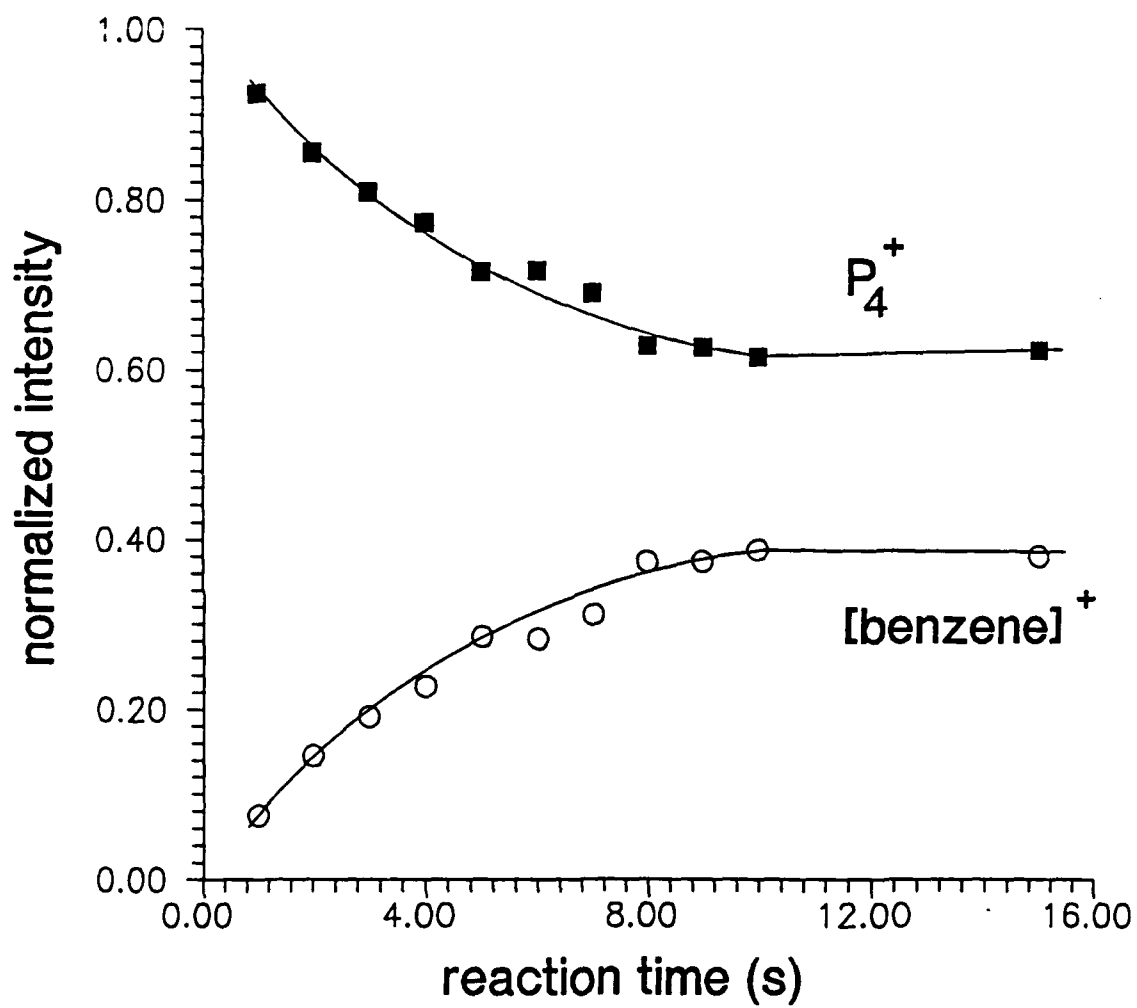
Figure 5. Normalized ion intensities of P₄⁺ and C₆H₆⁺ vs. reaction time for the reaction P₄⁺ + C₆H₆ → P₄ + C₆H₆⁺.











TECHNICAL REPORT DISTRIBUTION LIST - GENERAL

Office of Naval Research (2)
Chemistry Division, Code 1113
800 North Quincy Street
Arlington, Virginia 22217-5000

Commanding Officer (1)
Naval Weapons Support Center
Dr. Bernard E. Douda
Crane, Indiana 47522-5050

Dr. Richard W. Drisko (1)
Naval Civil Engineering
Laboratory
Code L52
Port Hueneme, CA 93043

David Taylor Research Center (1)
Dr. Eugene C. Fischer
Annapolis, MD 21402-5067

Dr. James S. Murday (1)
Chemistry Division, Code 6100
Naval Research Laboratory
Washington, D.C. 20375-5000

Defense Technical Information Center (2)
Building 5, Cameron Station
Alexandria, VA 22314

Dr. Robert Green, Director (1)
Chemistry Division, Code 385
Naval Weapons Center
China Lake, CA 93555-6001

Chief of Naval Research (1)
Special Assistant for Marine
Corps Matters
Code 00MC
800 North Quincy Street
Arlington, VA 22217-5000

Dr. Bernadette Eichinger (1)
Naval Ship Systems Engineering
Station
Code 053
Philadelphia Naval Base
Philadelphia, PA 19112

Dr. Sachio Yamamoto (1)
Naval Ocean Systems Center
Code 52
San Diego, CA 92152-5000

Dr. Harold H. Singerman (1)
David Taylor Research Center
Code 283
Annapolis, MD 21402-5067